

Segmentation by surface-to-image registration

Zhiyong Xie^a, Jose Tamez-Pena^b, Michael Gieseg^a, Serguei Liachenko^a, Shantanu Dhamija^a,
Ping Chiao^a

^aPfizer Inc, Ann Arbor, MI 48105, USA ^bVirtualScopics Inc, Rochester, NY 14625, USA

ABSTRACT

This paper presents a new image segmentation algorithm using surface-to-image registration. The algorithm employs multi-level transformations and multi-resolution image representations to progressively register atlas surfaces (modeling anatomical structures) to subject images based on weighted external forces in which weights and forces are determined by gradients and local intensity profiles obtained from images. The algorithm is designed to prevent atlas surfaces converging to unintended strong edges or leaking out of structures of interest through weak edges where the image contrast is low. Segmentation of bone structures on MR images of rat knees analyzed in this manner performs comparably to technical experts using a semi-automatic tool.

Keywords: Deformable Geometry, Segmentation, Registration, Magnetic Resonance, Orthopedic

1. INTRODUCTION

Magnetic resonance imaging (MRI) provides a noninvasive way to assess osteoarthritis (OA) progression in both human and animals. OA has been shown to be associated with cartilage degradation and thinning.¹ To quantify cartilage losses due to degradation and thinning, it is essential to be able to accurately segment the cartilage. Several groups have proposed two-step methods to segment articular cartilage. First, the easily identified bone structures such as tibia and femur are segmented. Second, the segmented tibia and femur are used to guide the segmentation of cartilage.^{2,3} In a longitudinal study, bone structures can also be used to register baseline and follow-up cartilages such that regional analysis of changes can be carried out. However, bone segmentation is a challenging problem by itself. This is even more so when small animals are used in pre-clinical imaging studies where both signal-to-noise ratios and contrast are mediocre.

Image segmentation is a process of grouping and labeling voxels that belong to the same anatomical structures. This can be achieved by detecting boundaries of the structure or by classifying every voxel based on its intensity properties (refer to the overviews of Duncan *et al.*⁴ and Pham *et al.*⁵ for current methods in medical image segmentation). Among all image segmentation methods, active contour^{6,7} and level set⁸ have received more and more attention and have been applied to segment MRI bone structures.⁹ These methods work by iteratively fitting a deformable model that is constrained in shape to a structure. To avoid erroneous convergence, shape priors are employed to guide the surface evolution. For example, Stib and Duncan incorporated global shape information in their deformable models.¹⁰ Cootes *et al.* and Leventon *et al.* used a statistical shape model derived from training data to constrain the solution.^{11,12} Yang and Duncan employed joint prior knowledge of structure shapes and image intensity to aid the segmentation.¹³ Cootes *et al.* and Kelemen *et al.* derived statistical models of both shape and appearance (intensity around the boundary) from training data to regulate the shape deformation.^{14,15} Excellent reviews for deformable models used in medical image analysis have been presented by McInerney *et al.*¹⁶ and Xu *et al.*¹⁷

Segmentation can also be achieved by registering a subject image to a reference image. To segment individual subject images, an atlas is produced by delineating and labeling anatomical regions of interest (ROIs) on the reference image. This atlas-based segmentation approach has been implemented to use intensity information to

Further author information: (Send correspondence to Zhiyong Xie)

Zhiyong Xie: zhiyong.xie@pfizer.com. This work was carried out at VirtualScopics Inc.

Jose Tamez-Pena: jose_tamez@virtualscopics.com

Serguei Liachenko: Serguei.Liachenko@pfizer.com

Shantanu Dhamija: Shantanu.Dhamija@pfizer.com

Ping Chiao: ping-chun.chiao@pfizer.com

compute a deformable transformation between the reference and subject images.¹⁸⁻²¹ The deformable transformation can subsequently be used to map any ROI defined on the atlas to the subject image. This approach can not only segment ROIs on each subject image, but also provide a mapping between reference and subject images. This mapping can enable quantitative regional analysis across different subjects or in the same subject at different times. However, atlas-based segmentation using intensity information does not work well for MR images of rat knee because the intensity within the bone is not uniform.

In this paper, we describe a new approach to atlas-based segmentation. Instead of using intensity-based registration, we register the surface extracted from the atlas to subject images. i.e., a transformation is computed to match atlas surfaces to edges on subject images. To allow for deformable transformation, we use a deformable model to characterize the surface. To support robust computation, we use multi-level transformations (rigid, affine, and multi-level B-splines) to progressively fit the deformable surface to each subject image.²²⁻²⁴ In addition, we use intensity patterns around boundaries of ROI to guide the fitting process. To speed up computation, we employ the multi-resolution scheme.²⁵ Experiments and validation studies using MRI images of rat knee demonstrate promising results.

This paper is organized as follows. Section 2 outlines our method for registering atlas surface to subject image. Experimental results and validation studies are presented in section 3 and section 4, respectively. Conclusion is given in section 5.

2. ALGORITHM

Supposed an atlas is created by delineating and labeling the anatomical structures on a reference image. Let S be a surface mesh extracted from an anatomical ROI on the atlas. I is an image to be segmented (For convenience, we call the reference image as atlas image. The image to be segmented as subject image). Our objective is to find a deformable transformation \mathbf{T} to fit S to the corresponding anatomical region shown on I .

There are numerous methods to compute a deformable transformation \mathbf{T} . A popular approach is to define a metric such as an energy measure and use optimization methods to find \mathbf{T} by minimizing the energy. For instance, energy can be defined as

$$\mathbf{E}(\mathbf{T}) = - \sum_{\mathbf{v}_i \in S} |\nabla I(\mathbf{T}(\mathbf{v}_i))|^2, \quad (1)$$

where $\nabla I(\mathbf{x})$ is the gradient of image I at point \mathbf{x} .

To optimize this kind of energy, an iterative procedure can be used to compute the transformation \mathbf{T} so that $\mathbf{T}(S)$ best fit to high gradient points on image I :

1. For each point \mathbf{v}_i on atlas surface S , search for the point \mathbf{p}_i along normal vector of \mathbf{v}_i where \mathbf{p}_i has the greatest magnitude of gradient.
2. Compute the parameters of transformation \mathbf{T} such that $\sum_i \|\mathbf{T}(\mathbf{v}_i) - \mathbf{p}_i\|^2$ is minimized.
3. Update all points on surface S by setting $\mathbf{v}_i = \mathbf{T}(\mathbf{v}_i)$.

There are two problems with this approach. First, only magnitudes of gradient are used in this system. Omitting other image features may make the fitting process unstable and could potentially cause S to converge to a wrong solution. Another problem is the selection of the transformation. Without any constraint on transformation \mathbf{T} , the fitting will be ill-posed because an infinite number of solutions can be found. Similar to image registration and surface matching, it is desirable to best fit S to I with the least deformation in \mathbf{T} .²⁶

To address the first problem, intensity profile proposed by Cootes *et al.*¹⁴ and Kelemen *et al.*¹⁵ are incorporated in our approach. Instead of finding the point with greatest magnitude of gradient, the best matched point, where the intensity profile is most similar to the intensity profile of atlas point, is identified to compute the transformation. Intensity profile of a point \mathbf{v}_i on atlas surface S (which is called atlas profile) is defined as intensities of a discrete set of sampling points on the atlas image along normal direction \mathbf{n}_i centered at \mathbf{v}_i .

To search for the best matching point on the subject image, sampling points of atlas profile are shifted along \mathbf{n}_i and their intensities on the subject image is retrieved as subject profile and compared to atlas profile. The point with most similar profiles are selected as the best matching point. In our approach, similarity between two profiles are defined as a combination of correlation coefficient of two profiles and the angle between normal vector \mathbf{n}_i and gradient vector \mathbf{g} of found point \mathbf{q} on subject image. In our application of bone segmentation on MRI T1-weighted images, the intensities of bone structure are always lower than the soft tissues surrounding the structure. If \mathbf{q} is the corresponding point of \mathbf{v}_i , the direction of gradient vector \mathbf{g} should be similar to the normal vector \mathbf{n}_i . In this application, similarity between atlas surface point \mathbf{v}_i and a sought point \mathbf{q} is defined as

$$s = \begin{cases} \cos(\theta)C(\mathbf{v}_i, \mathbf{q}) & \text{if } \cos(\theta) \geq 0. \\ 0 & \text{otherwise.} \end{cases} \quad (2)$$

where θ is the angle between normal vector \mathbf{n}_i and gradient vector \mathbf{g} . $C(\mathbf{v}_i, \mathbf{q})$ is the correlation coefficient of atlas intensity profile at \mathbf{v}_i and subject intensity profile at \mathbf{q} .

To address the second problem, multi-level transformations are employed to reduce the effect of over deformation and the possibility of erroneous convergence. Multi-level transformations have been widely used in image registration and surface-to-surface matching^{22,23,27,28} for the exact same purpose. In our approach, a rigid transformation is first computed to fit S to I . The result is used to initialize an affine transformation. Finally, a deformable transformation, in which the number of degrees of freedom is gradually increased, is computed to refine the result. Our algorithm is outlined as follows:

1. \mathbf{T} is a transformation with unknown parameters. \mathbf{v}_i is *ith* point on S .
2. In each iteration, search along normal vector of \mathbf{v}_i in a predefined region in I with step size of half pixel. Let $\mathbf{p}_i = \mathbf{q}$ and $w_i = s$ where \mathbf{q} is the point with the greatest similarity s to point \mathbf{v}_i among all sought points.
3. Compute the parameters of transformation \mathbf{T} such that $\sum_i w_i \|\mathbf{T}(\mathbf{v}_i) - \mathbf{p}_i\|^2$ is minimized.
4. Update all points on surface S by setting $\mathbf{v}_i = \mathbf{T}(\mathbf{v}_i)$.
5. Repeat steps 2 through 5 if \mathbf{T} is not closed to an identity transformation.
6. Stop if $\sum_i w_i \|\mathbf{T}(\mathbf{v}_i) - \mathbf{p}_i\|^2 < \epsilon$ while ϵ is a predefined threshold. Otherwise, increase the degree of freedom in transformation \mathbf{T} , reduce the searching range, and repeat steps 2 through 6.

In step 3, \mathbf{T} is computed in the following order: rigid transformation, affine transformation, and deformable transformation. For rigid transformation, parameters are computed using Singular Value Decomposition (SVD).²⁹ For affine transformation, the least squares solutions are computed. To compute the deformable transformation, multi-level B-splines, in which the number of B-spline control points is increased gradually, are used to progressively refine the result. An efficient B-spline approximation algorithm proposed by Lee *et al.*³⁰ is employed to compute these control points.

In this system, the force generated at each point of atlas surface has weighted contribution to the computation of the transformation. If a point at atlas surface is not sure whether the found matching point is the ideal target, it should make less contribution to the computation of transformation than the points with more confidence. For those points with weight zero, they will make no contribution to the computation of transformation and just move along with other points.

To reduce the possibility for surface points to leak out of the anatomical region of interest through a weak edge (where the image gradient is small and edge contrast is poor), searching ranges of edges points in step 2 are limited to small regions adjacent to the atlas surface as the number of B-spline control points is gradually increased. This scheme also prevents surface points adjacent to low contrast regions from being attracted by edges of neighboring structures.

To speed up computation and convergence, a multi-resolution scheme, which is widely used in intensity-based image registration,²⁵ is employed in our surface-to-image registration. In our implementation, an image pyramid is created using a procedure provided in ITK (Insight Segmentation and Registration Toolkit,



Figure 1. Example of tibia segmentation. Original overlap of tibia contour of atlas on subject image (left), Overlap after rigid transformation which moves the contour closer to the tibia structure of subject (middle), and final result after B-Spline deformation (right).

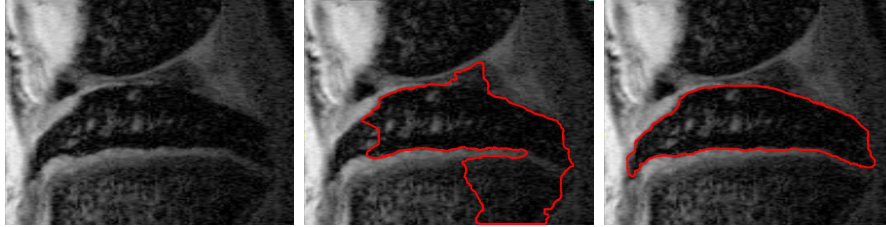


Figure 2. Segmentation on the weak edge. Image with a weak edge (left), bleeding problem (middle), and segmentation result using proposed method (right).

<http://www.itk.org>) which performs the smoothing followed by down sampling to generate lower resolution images.

Since a smooth transformation is used to map atlas surfaces to subject structures, some small regions around the structures which are not smooth may be misclassified. To address this problem, a relaxation is performed to correct such misclassification. We employ a Gibbs random field to reclassify and relabel each voxel.³¹

3. EXPERIMENTS

Thirty-six T1-weighted MR images of rat knees were used to evaluate the proposed algorithm (size: $128 \times 152 \times 36$, resolution: $0.063 \times 0.035 \times 0.25$ mm). All image sets were processed using both our implemented algorithm and a classification-based semi-automatic tool. Visual inspection determined that only 3 of 36 (8%) images using our implemented algorithm required minor manual corrections as opposed to 36 of 36 using the semi-automatic tool. Figure 1 demonstrates that the method can successfully register an atlas surface to the targeted tibia despite the fact that the atlas surface crosses strong edges of neighboring structures in the initial position (picture on the left), which usually imposes difficulties for such convergence. The middle picture shows the result after rigid transformation; the atlas surface has moved closer to the tibia structure. The right picture shows final result after the B-Spline deformable transformation. The average runtime for these experiments was 5 minutes on a 2.8GHz Pentium PC (Windows 2000, 2GB RAM).

The proposed algorithm also works in regions having weak edges. Weak edges usually causes bleeding problems where the deformable surface may leak into adjacent structures (see figure 2). To minimize the impact of weak edges, our algorithm assigns small weights to surface points adjacent to low contrast areas. This scheme prevents the atlas surface from leaking out of structures of interest through weak edges.

4. VALIDATION

To validate our algorithm, 3 data sets from different rats were segmented using a semi-automated system developed by VirtualScopics.³¹ For each data set, an unsupervised statistical segmentation followed by manual editing was performed by four trained experts. The results generated by the proposed algorithm were compared with those generated by experts using the semi-automated approach. Since there was no ground truth available

Table 1. Segmentation performance of proposed algorithm and experts

<i>Data</i>	<i>Algorithm</i>		<i>Expert 1</i>		<i>Expert 2</i>		<i>Expert 3</i>		<i>Expert 4</i>	
	p	q	p	q	p	q	p	q	p	q
data 1	1.000	0.974	1.000	1.000	0.998	1.000	0.999	0.996	0.992	1.000
data 2	1.000	0.980	1.000	0.998	0.981	1.000	1.000	0.998	0.981	1.000
data 3	0.998	0.982	1.000	0.996	0.979	1.000	1.000	0.996	0.980	1.000
Average	1.000	0.979	1.000	0.998	0.986	1.000	1.000	0.997	0.984	1.000

in this validation study, the method proposed by Warfield *et al.*³² was used to evaluate the performances of both approaches. This method employs the Expectation-Maximization algorithm to compute an estimate of the “ground truth” as well as the sensitivity and specificity of each reader in delineating and labeling the tibia structure. Here we treat our algorithm as an independent reader. The sensitivity p (relative frequency of $D_i = 1$ when $T_i = 1$, where D_i is the segmentation on voxel i , and T_i is ground truth of voxel i) and specificity q (relative frequency of $D_i = 0$ when $T_i = 0$) of proposed algorithm and four experts are presented in table 1. The proposed algorithm compares favorably to experts using the semi-automated approach in sensitivity, while it performs slightly behind the experts in specificity.

5. CONCLUSION

An automated approach to registration and segmentation of the rat tibia on MR images has been developed. Experimental results demonstrate that this approach can prevent atlas surface converging to a strong edge of neighboring structures, or leaking out of structure of interest through weak edge. Validation studies show that this approach performs very close to experts using semi-automated approach.

In the systems proposed by Cootes *et al.*¹⁴ and Kelemen *et al.*,¹⁵ both shape and intensity models are constructed based on training data sets. Shape model is created using Principal Component Analysis (PCA) approach. The mean shape of training data is used as atlas surface. The mean intensity profile and covariance matrix of intensity profiles from training data are used as the intensity model of atlas. Mahalanobis distance of a new intensity profile to the mean intensity profile is used to determined the similarity between the new intensity profile and the atlas intensity profile. In our approach, we just select a single image as atlas, and use correlation coefficient to measure the similarity between intensity profiles. This is based on the consideration that our acquisition protocol may change from time to time. Using single image as atlas makes it easier to pick up a new atlas for the data with new intensity pattern.

The proposed approach not only segments the anatomical region of interest, but also generates a spatial mapping between corresponding regions, providing more versatile information that can not be easily obtained using active contour or level set algorithms. In contrast to the conventional atlas-based segmentation method using intensity-based registration, our approach employs surface-to-image registration, which is less sensitive to structure differences between atlas and image data in the regions other than ROI boundary. In conclusion, our deformable surface-to-image registration approach has demonstrated promising results in the analysis of MR images of rat knees. Future work includes extracting shape priors from existing data, and use this information to guide registration between atlas surfaces and individual images.

REFERENCES

1. F. Eckstein, M. Reiser, K.-H. Englmeier, and R. Putz, “In vivo morphometry and functional analysis of human articular cartilage with quantitative magnetic resonance imaging - from image to data, from data to theory,” *Anatomy and Embryology* **203**(3), pp. 147–173, 2001.
2. S. Pakin, J. Tamez-Pena, and S. T. K. Parker, “Segmentation, surface extraction, and thickness computation of articular cartilage,” in *SPIE Medical Imaging*, pp. 155–166, 2002.

3. T. Kapur, P. A. Beardsley, S. F. Gibson, W. E. L. Grimson, and W. M. Wells, "Model based segmentation of clinical knee MRI," in *Model-based 3D Image Analysis (in conjunction with ICCV)*, (Bombay, India), Jan 1998.
4. J. Duncan and N. Ayache, "Medical image analysis: Progress over two decades and the challenges ahead," *IEEE Transactions on Pattern Analysis and Machine Intelligence* **22**(1), pp. 85–106, 2000.
5. D. L. Pham, C. Xu, and J. L. Prince, "Current methods in medical image segmentation," in *Annual Review of Biomedical Engineering*, **2**, pp. 315–337, 2000.
6. M. Kass, A. Witkin, and D. Terzopoulos, "Snakes: Active contour models," *International Journal of Computer Vision* **1**, pp. 312–331, 1988.
7. L. Cohen and I. Cohen, "Finite-element methods for active contour models and balloons for 2-d and 3-d images," *IEEE Transactions on Pattern Analysis and Machine Intelligence* **15**(11), pp. 1131–1147, 1993. URL: <http://citeseer.nj.nec.com/cohen91finite.html>.
8. S. Osher and J. A. Sethian, "Fronts propagating with curvature-dependent speed: algorithms based on hamilton-jacobi formulations," *Journal of Computational Physics* **79**(1), pp. 12–49, 1988.
9. L. Lorigo, O. Faugeras, W. Grimson, R. Keriven, and R. Kikinis, "Segmentation of bone in clinical knee mri using texture-based geodesic active contours.," in *Medical Image Computing and Computer-Assisted Intervention*, October 1998.
10. L. H. Staib and J. S. Duncan, "Boundary finding with parametrically deformable models," *IEEE Trans. Pattern Anal. Mach. Intell* **14**(11), pp. 1061–1075, 1992.
11. T. F. Cootes, A. Hill, C. J. Taylor, and J. Haslam, "The use of active shape models for locating structures in medical images," *Image and Vision Computing* **12**(6), pp. 355–366, 1994.
12. M. Leventon, W. Grimson, and O. Faugeras, "Statistical shape influence in geodesic active contours," in *IEEE Conf. Comp. Vision and Patt. Recog*, pp. 316–323, 2000.
13. J. Yang and J. S. Duncan, "3d image segmentation of deformable objects with shape-appearance joint prior models using level sets," *Medical Image Analysis* **8**(3), pp. 285–295, 2004.
14. T. Cootes and C. Taylor, "Statistical models of appearance for medical image analysis and computer vision," in *Proc. SPIE Medical Imaging*, 2001.
15. A. Kelemen, G. Székely, and G. Gerig., "Elastic model-based segmentation of 3-d neuroradiological data sets," *IEEE Trans. on Medical Imaging* **18**, Oct 1999.
16. T. McInerney and D. Terzopoulos, "Deformable models in medical images analysis: a survey," *Medical Image Analysis* **1**(2), pp. 91–108, 1996.
17. C. Xu, D. L. Pham, and J. L. Prince, "Medical image segmentation using deformable models," in *Handbook of Medical Imaging – Volume 2: Medical Image Processing and Analysis*, J. Fitzpatrick and M. Sonka, eds., pp. 129–174, SPIE Press, 2000.
18. D. L. Collins, W. Dai, T. M. Peters, and A. C. Evans, "Model-based segmentation of individual brain structures from MRI data," in *Visualization in Biomedical Computing 1992: Proc SPIE*, pp. 10–23.
19. J. Haller, G. Christensen, S. Joshi, M. Miller, and M. Vannier, "Digital atlas-based segmentation of the hippocampus," in *Computer Assisted Radiology*, H. Lemke, K. Inamura, C. Jaffe, and J. W. Vannier, eds., pp. 152–157, Springer Verlag, Berlin, June 1995.
20. S. Warfield, A. Robatino, J. Dengler, F. Jolesz, and R. Kikinis, "Nonlinear registration and template-driven segmentation," in *Brain Warping*, W. Toga, ed., pp. 67–84, Academic Press, 1998.
21. J. Gee, M. Reivich, and R. Bajcsy, "Elastically deforming 3D atlas to match anatomical brain images," *J Comput Assist Tomogr* **17**, pp. 225–236, 1993.
22. K. Friston, J. Ashburner, C. Frith, J.-B. Poline, J. Heather, , and R. Frackowiak, "Spatial registration and normalization of images," **2**, pp. 165–189, 1995.
23. R. Woods, "Automated global polynomial warping," in *Brain Warping*, W. Toga, ed., pp. 365–376, Academic Press, 1998.
24. Z. Xie, L. Ng, and J. Gee, "Two algorithms for non-rigid image registration and their evaluation," in *Proceedings of SPIE on Medical Imaging 2003, San Diego*, 2003.
25. S. Kovacic and R. Bajcsy, "Multiscale/multiresolution representations," in *Brain Warping*, W. Toga, ed., pp. 45–65, Academic Press, 1998.

26. S. Joshi, B. Davis, M. Jomier, and G. Gerig, "Unbiased diffeomorphic atlas construction for computational anatomy," *NeuroImage* **23**(Supplement 1), pp. S151–S160, 2004.
27. Z. Xie and G. E. Farin, "Image registration using hierarchical B-splines," *IEEE Trans. Vis. Comput. Graph* **10**(1), pp. 85–94, 2004.
28. J. Feldmar and N. Ayache, "Rigid, affine and locally affine registration of free-form surfaces," Tech. Rep. 2220, Institut National de Recherche en Informatique et en Automatique, 1994. URL: <http://www.inria.fr/RRRT/RR-2220.html>.
29. K. S. Arun, T. S. Huang, and S. D. Blostein, "Least-squares fitting of two 3-d point sets," *IEEE Trans. Pattern Anal. Mach. Intell.* **9**(5), pp. 698–700, 1987.
30. S. Lee, G. Wolberg, and S. Y. Shin, "Scattered data interpolation with multilevel B-Splines," *Visualization & Computer Graphics* **3**(3), pp. 228–244, 1997.
31. J. Tamez-Pena, K. J. Parker, and S. Totterman, "Unsupervised statistical segmentation of multispectral volumetric MR images," in *Proceedings of SPIE Medical Imaging*, 1999.
32. S. Warfield, K. Zou, and W. Wells, "Simultaneous truth and performance level estimation (staple): An algorithm for the validation of image segmentation," *IEEE TRANSACTIONS ON MEDICAL IMAGING*, **23**, pp. 903–921, July 2004.